Original article

Abnormal mitochondrial function impairs calcium influx in diabetic mouse pancreatic beta cells

LI Fei, D. Marshall Porterfield, ZHENG Xi-yan, WANG Wen-jun, XU Yue and ZHANG Zong-ming

Keywords: *type 2 diabetes; pancreatic beta cell; insulin secretion; Ca^{2+} influx; mitochondrial function*

Background Abnormal insulin secretion of pancreatic beta cells is now regarded as the more primary defect than the insulin function in the etiology of type 2 diabetes. Previous studies found impaired mitochondrial function and impaired Ca^{2+} influx in beta cells in diabetic patients and animal models, suggesting a role for these processes in proper insulin secretion. The aim of this study was to investigate the detailed relationship of mitochondrial function, Ca^{2+} influx, and defective insulin secretion.

Methods We investigated mitochondrial function and morphology in pancreatic beta cell of diabetic KK-Ay mice and C57BL/6J mice. Two types of Ca^{2+} channel activities, L-type and store-operated Ca^{2+} (SOC), were evaluated using whole-cell patch-clamp recording. The glucose induced Ca^{2+} influx was measured by a non-invasive micro-test technique (NMT).

Results Mitochondria in KK-Ay mice pancreatic beta cells were swollen with disordered cristae, and mitochondrial function decreased compared with C57BL/6J mice. Ca^{2+} channel activity was increased and glucose induced Ca^{2+} influx was impaired, but could be recovered by genipin.

Conclusion Defective mitochondrial function in diabetic mice pancreatic beta cells is a key cause of abnormal insulin secretion by altering Ca^{2+} influx, but not via Ca^{2+} channel activity.

Chin Med J 2012;125(3):502-510

Type 2 diabetes is characterized by impaired insulin action and secretion.[1,2] The relative importance of insulin action and secretion in disease progression has been hotly debated. Historically, type 2 diabetes has been considered a disease of insulin resistance, but it is now recognized that abnormal insulin secretion is a key element in the development of the disease.[2,3]

In pancreatic beta cells, mitochondria and Ca^{2+} influx play a critical role in regulating glucose stimulated insulin secretion (GSIS) that is the major mechanism for insulin release. After glucose is transported into the cytosol and metabolized into pyruvate by glycolysis, mitochondria metabolize pyruvate to produce adenosine triphosphate (ATP) and other metabolic products via the tricarboxylic acid (TCA) cycle.[4,5] ATP can trigger closure of ATP-sensitive potassium channel (K_{ATP} channel) attributed to membrane depolarization. Besides acting on the K_{ATP} channel, ATP interacts with other products of mitochondria metabolism that have been proposed to increase production of inositol 1,4,5-trisphosphate (IP_3),[6] which in turn mobilizes Ca^{2+} from the endoplasmic reticulum (ER).[7,8] Ca^{2+} mobilization activates store-operated Ca^{2+} channel (SOC),[9] and this current cooperates with the closure of K_{ATP} channel, resulting in membrane depolarization and activation of voltage-dependent Ca^{2+} channel (VDCC). L-type Ca^{2+} channels are considered the most important Ca^{2+} entry pathway that controls insulin secretion in all beta cells and cell lines.[10] This Ca^{2+} signal triggers insulin secretion. Thus, mitochondria activation and Ca^{2+} channel activity are two crucial factors in the GSIS of beta cells.

Mitochondria not only produce ATP for basic physiological activity but also affect insulin secretion in pancreatic beta cells. Mitochondria were originally associated with pathogenesis of type 2 diabetes because of the mitochondrial DNA mutations observed in human diabetes. Therefore, most studies on mitochondria focused on the relationship of insulin resistance with peripheral organs such as liver and skeletal muscle. Insulin resistance alone, however, cannot be responsible for the onset of type 2 diabetes. Further study found

DOI: 10.3760/cma.j.issn.0366-6999.2012.03.019
Department of General Surgery, Digestive Medical Center, the First Affiliated Hospital, Medical School, Tsinghua University, Beijing 100016, China (Li F, Zheng XY and Zhang ZM)
Birck Bindley Bioscience Center, Department of Agricultural and Biological Engineering, Department of Horticulture and Landscape Architecture, Weldon School of Biological Engineering, Purdue University, West Lafayette, IN 47906, USA (Porterfield DM)
Beijing Science & Technology Co., Ltd., Beijing 100080, China (Wang WJ and Xu Y)
Correspondence to: ZHANG Zong-ming, Department of General Surgery, Digestive Medical Center, the First Affiliated Hospital, Medical School, Tsinghua University, Beijing 100016, China (Tel: 86-10-64372362. Fax: 86-10-64361322. Email: zhangzongming@mail.tsinghua.edu.cn)
This study was supported by grants from Fund of Capital Medical Development and Research (No. 2009-1020) and Tsinghua-Yue-Yuen Medical Science Foundation (No. 20240000531 and No. 20240000568)
The authors declare that there is no conflict of interest associated with this manuscript.

pancreatic beta cell specific deletion of mitochondrial genes in animal models can cause diabetes[11,12] and the importance of ATP production to insulin secretion was verified by mutating the K_{ATP} channel.[13] In recent studies, abnormal mitochondria morphology and function was observed in type 2 diabetic patients, and was associated with abnormal insulin secretion in diabetic mice.[14-17] However, there was still no data on how abnormal mitochondrial function affects insulin secretion. At the same time, calcium as the most important second messenger engaged in various pathophysiologic activities and also acts as a pivotal role in insulin secretion. In the GSIS, the major way of Ca^{2+} influx is though the L-type Ca^{2+} channel. In beta cell-specific subunits of L-type Ca^{2+} channel null mice, insulin secretion and glucose tolerance were impaired[18] and we found subunits of L-type Ca^{2+} channel expression of beta cell line increased in our previous study.[19] Although the Ca^{2+} release-activated Ca^{2+} influx apparently accounts for a minor fraction of normal Ca^{2+} entry into beta cells, it could be significant as a depolarizing factor involving the activation of L-type Ca^{2+} channel.[20] The data indicated that long-term changes of store operated Ca^{2+} influx may underlie disturbances of beta cell function. Other studies found impaired Ca^{2+} oscillations result in deficiencies in insulin secretion in certain forms of type 2 diabetes in humans and rodents,[21,22] but the mechanism remains unclear. Thus, the link between mitochondria, Ca^{2+} influx and defective insulin secretion has not been established.

In the present study, we aimed to study whether abnormalities in insulin release found in type 2 diabetes is secondary to Ca^{2+} signaling changes caused by abnormal mitochondria function.

METHODS

Animals

We chose KK-Ay mice as the type 2 diabetes animal model and C57BL/6J mice as healthy controls. Male C57BL/6J and KK-Ay mice at age of 8–10 weeks were obtained from the Chinese Academy of Medical Sciences. Each mouse was housed in an individual cage, and in an environmentally controlled condition with a 12 hour light/dark cycle. All mice had free access to rodent pellet food (Chinese Academy of Medical Sciences) and water ad libitum, except for when restrained before the experiments. After being acclimated to the environment for one week, KK-Ay mice with stable fasting blood glucose levels greater than 16 mmol/L (Bionime Rightest GM300 Blood Glucose Monitoring Kit), were selected for subsequent experiments. All mice were housed and cared for according to the approved protocols of the Tsinghua University Animal Care and Use Committee.

Islet isolation and insulin secretion

C57BL/6J and KK-Ay mice were sacrificed by cervical dislocation after fasting 12 hours, and pancreatic islets were isolated by collagenase digestion as previously described,[23,24] Intact islets were placed in a cell culture chamber overnight in RPMI 1640 supplemented with 10% fetal calf serum. Insulin release from islets was measured as previously described by radioimmunoassay as described previously.[25] In brief, groups of 20 islets of C57BL/6J and KK-Ay were pre-incubated in Krebs-Ringer buffer (in mmol/L: 115 NaCl, 5 KCl, 10 $NaHCO_3$, 1.2 KH_2PO_4, 1.1 $MgCl_2$, 2.5 $CaCl_2$, 3 glucose, 25 HEPES, pH 7.4) containing 0.5% bovine serum albumin (BSA) at 3 mmol/L glucose for 40 minutes. Islets were then incubated with 1 ml of Krebs-Ringer buffer with 0.5% BSA in 20 mmol/L glucose for 40 minutes. Subsequently, the media was replaced with fresh media. Total islet insulin levels were determined by extraction in 0.5 ml of cold acid ethanol mixture (75% ethanol with 0.2 mol/L HCl). Hoechst-33258 staining of sonicated islets was performed to determine the DNA content.

Ultrastructural islet analysis

Electron microscopic analysis was completed on islets isolated from six to eight mice per genotype essentially as described.[26] The samples were observed under the H-7650 HITACHI transmission electron microscope operating at 80 kV. Images were recorded digitally using an AMT camera system. Beta cells were recognized by their typical ultrastructural appearance. The area and number of beta cell mitochondrion were quantified by analyzing 50–100 images magnified 10 000× with electron microscope from random areas of islets, isolated from each mouse. Area and number were determined using the threshold setting and the particle analysis tool in Image J software (National Institutes of Health, Bethesda, MD, USA).

Mitochondrial membrane potential

Glucose stimulation results in the transfer of reducing equivalents to the respiratory chain, leading to hyperpolarization of the mitochondrial membrane ($\Delta\Psi m$), and generation of ATP. Rhodamine 123 (Rh123) was used to compare the mitochondrial potential changes in islet cells suspended in 20 mmol/L glucose. Briefly, islet cells were loaded in Krebs-Ringer buffer containing 3 mmol/L glucose and 10 μg/ml Rh123 for 30 minutes at 37°C. Cells were resuspended in the same buffer without Rh123 and transferred to a BD Aria flow cytometer (Franklin Lakes, NJ, USA), and fluorescence excited at 488 nm and measured at 530 nm. Fluorescent responses 15 minutes after addition 20 mmol/L glucose and 10 minutes of respiration inhibitor (10 mmol/L sodium azide) were compared with baseline (3 mmol/L glucose), and used to characterize mitochondrial depolarization and hyperpolarization, respectively. A decrease in fluorescence corresponded to an increase in $\Delta\Psi m$. The identification of beta cells was based on size. Results are expressed as percentage of basal fluorescence (at 3 mmol/L glucose).

Electrophysiology

Whole-cell patch-clamp recording was performed in a

computer-based patch-clamp amplifier (EPC-10, HEKA Electronics, Lambrecht/Pfalz, Germany), and PatchMaster software (HEKA Electronics, MAHONE Bay, Nova Scotia, Canada). The patch pipettes were pulled from borosilicate glass and fire polished. Pipette resistance ranged between 3 and 5 MΩ.

A standard external solution containing the following (in mmol/L): NaCl 120; $CaCl_2$ 2.5; HEPES 10; glucose 3; TEA-Cl 20; $MgCl_2$ 1 with osmolarity adjusted to around 310 mOsm (pH 7.4, adjusted with NaOH), and further supplemented with TTX 1 μm, SNX-482 200 nm, 100 μmol/L 4,4′-diisothiocyano-2,2′-stilbene disulphonic acid (DIDS). The internal solution for VDCC containing (in mmol/L): CsCl 125; $MgCl_2$ 1; EGTA 10; HEPES 10 (pH 7.2, adjusted with CsOH), and 2 μmol/L thapsigargin (Tg) was added to deplete Ca^{2+} stores for inducing store-operated Ca^{2+} influx. In whole cell experiments, recording started when the series resistance dropped below 20 MΩ. Dispersed islet cells grown in 35-mm dishes and only cells with a cell capacitance of >5 pF were analyzed, being most likely pancreatic beta cells.[27] We also performed single cell reverse transcription-polymerase chain reaction (RT-PCR) to identify cells measured by whole-cell patch-clamp recording.[28] Harvesting cytoplasm of patched cells was performed by a gentle suction applied to the pipette. The tip of the pipette was then broken in a PCR tube containing the required reagents for reverse transcription, which was followed by insulin specific primers of F-primer (CCAGTAACCCCCAGCCC) and R-primer (GCCACC-TCCAACGCCAA), and the length of production was 317 bp. The first PCR amplification was performed as follows: a pre-denaturation at 94°C for 3 minutes, followed by 25 cycles of denaturation at 94°C for 30 seconds, annealing at 57°C for 30 seconds, and synthesis at 72°C for 1 minute, and then a last extension step at 72°C for 1 minute. The second round of PCR was then performed using 5 μl of the product of the first amplification as the template. Then gene fragment was amplified individually using its specific primer pair and 35 cycles. PCR products were analyzed using agarose gel electrophoresis.

Voltage-dependent currents were corrected for linear leak and residual capacitance by use of an on-line P/n subtraction. The cells were held at –70 mV with test pulses ranging from –50 to 60 mV with 10 mV increments. For the normalized current recordings, peak currents were measured at 0 mV.

Store operated Ca^{2+} influx was detected using voltage ramps of 100 ms duration, spanning a range of –100 to +100 mV, delivered from a holding potential of 0 mV every 2 seconds over a period of 600–1000 seconds. The maximal currents at –100 mV were used for statistical analysis. All voltages were corrected for a liquid-junction potential of 13 mV. Capacitative currents were determined and compensated for automatically by the EPC-10 amplifier. Data analysis was conducted using IGOR Pro 5.01 (Wavemetrics, Portland, OR, USA).

Ca^{2+} influx of islets

We used the non-invasive micro-test technique (NMT)[29,30] (BIO-001A; YoungerUSA, Amherst, MA, ScienceWares, Falmouth, MA.) to directly measure electrophysiological flux of Ca^{2+} ions of islets. NMT has the basic ability to non-invasively measure various types of ions and small molecules *in situ*, with a high level of both temporal and spatial resolution. It had been used to investigate the relationship between oxygen consumption oscillations, calcium, and insulin secretion. Clonal pancreatic beta cells (HIT),[31] O_2 and Ca^{2+} flux in neuron[32] and electric currents at wounds in human skin in rodent cornea and skin.[33] NMT parameters for ion flux measurements were based on moving the selective ion microelectrode between two positions according to Fick's Law. The near-pole position of the probe was typically within a micron of the surface of the islet, and we used a preset excursion of 30 μm at a programmable frequency in the range of 0.3 to 0.5 Hz. The microelectrodes (2–4 μm aperture, XYPG120-2; Xuyue Sci. and Tech. Co., Ltd.) were pulled and silanized using the glass micropipettes, but first filled with a backfill solution of 100 mmol/L $CaCl_2$. The backfill solution was pushed into the tip, and occupied a length of approximately 1 cm from the tip. Then the microelectrode was front filled with a column of a selective liquid ion-exchanger cocktail (LIX) imparting ion-selectivity, where the column length of Ca^{2+} was 15–20 μm. The LIX cocktail was purchased pre-made from Sigma-Aldrich (St. Louis MO, USA). The filled microelectrode was mounted in a microelectrode holder that facilitated a wire, acting as the electrical interface with the microelectrode through insertion into the backfill solution. The reference electrode was also a Ag/AgCl counter electrode, which was maintained in solution by a solid manipulator support. The ion electrodes were calibrated according to standard protocol and only those with Nernstian slopes (>50 mV/decade/monovalent; >25 mV/decade for Ca^{2+}) were used in our experiment. Ion flux was calculated by Fick's law of diffusion: J= –D (dc/dr), where J represents the ion flux (10^{-12} moles·cm^{-2}·s^{-1}), dc is the ion concentration difference (10^{-3} mol/L), dr is distance between two measured points (μm), and D is the ion diffusion constant in a particular solution and temperature (cm^2/s). Probe moment, data recording, digital image acquisition, and calibrations were performed with ASET software.

Ion flux conversion was obtained using Mageflux (YoungerUSA, Youngerusa, USA). Because the actual velocity of each islet varies with its size, and islets sizes range from 70 μm to 600 μm, the ionic fluxes were normalized and presented as the changes to basal flux by V_1/V_0, where V_0 is the average basal flux of each islet and V_1 is the actual flux. Positive values represent efflux, whereas negative values represent influx. Flux data were validated using the digital differential filtering (DDF) technique developed by McLamore et al.[34,35]

Statistical analysis

Results are expressed as mean ± standard error (SE). Statistical significance was assessed using either a Student's *t* test or one-way analysis of variance (ANOVA) for repeated measures, followed by multiple Bonferroni comparisons. P <0.05 was considered statistically significant difference.

RESULTS

Insulin secretion

As shown in Figure 1, 20 mmol/L glucose-stimulated insulin release was significantly lower from age matched KK-Ay compared with C57BL/6J islets ((537±87) pg/ng DNA per hour vs. (1187±167) pg/ng DNA per hour, P <0.01). These data indicate a secretion defect in type 2 diabetes beta cells in response to glucose stimulation.

Mitochondrial morphology in beta cells

We documented changes in mitochondrial morphology in beta cells of age matched healthy and diabetic mice using electron microscopy. Notably, the mitochondria in beta cells in KK-Ay mouse were often swollen, and the inner membranes of mitochondria were drastically disrupted with abnormal cristae (Figure 2A). The quantitative analysis revealed beta cells in KK-Ay mice contained significantly fewer mitochondria and were just 36.35% of healthy mice (P <0.01). However, the average area of mitochondria in diabetic KK-Ay mice was about 310% larger (P <0.01) compared with healthy controls (Figure 2B).

Mitochondrial membrane potential

A proton gradient across the inner mitochondrial membrane is produced by oxidative phosphorylation, which hyperpolarizes the mitochondrial membrane and drives ATP synthesis. Therefore, we measured changes in ΔΨm in beta cells using Rh123 under glucose stimulation to represent the mitochondrial function. Addition of 20 mmol/L glucose and 10 mmol/L of the respiratory inhibitor NaN_3 completely depolarized ΔΨm (decreased Rh123 fluorescence) (Figure 3). There was a significant

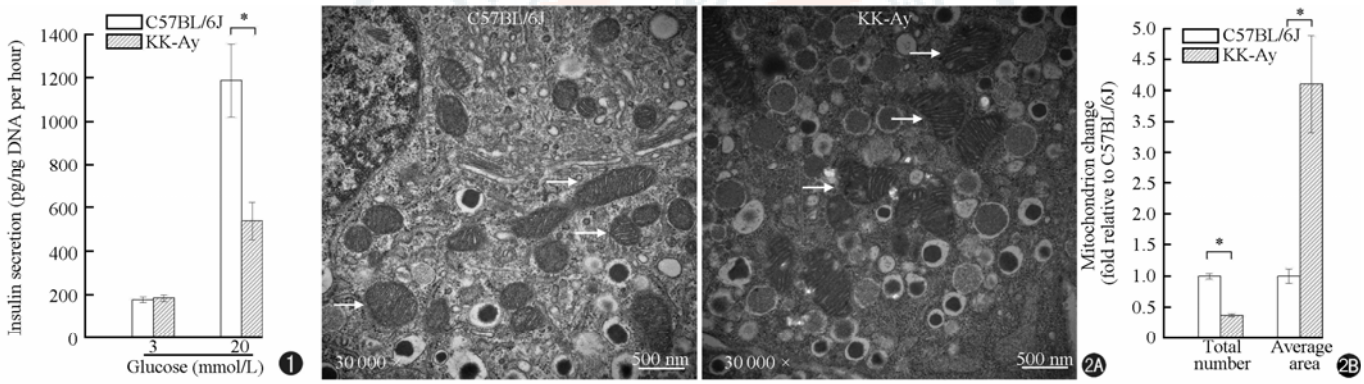

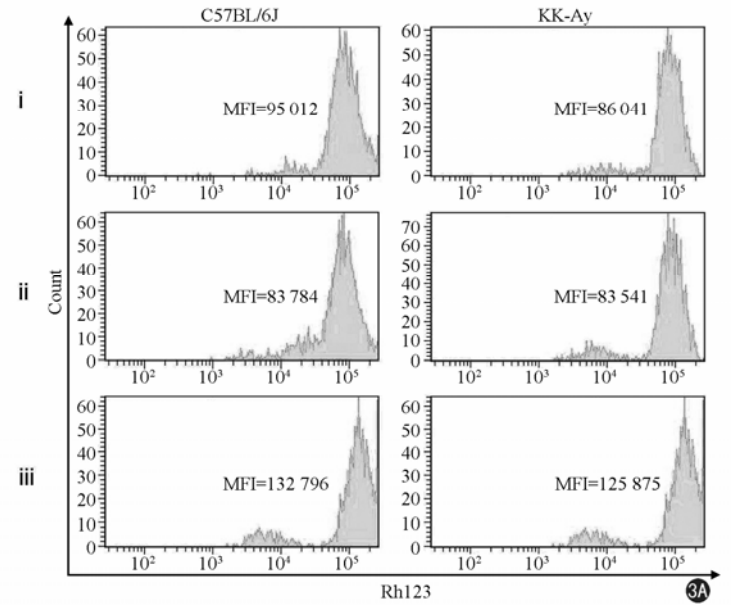

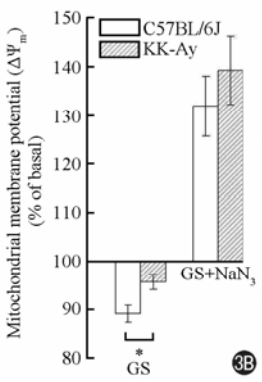

Figure 1. Glucose-stimulated insulin secretion in islets. Islets from age-matched KK-Ay and C57BL/6J mice were exposed to 3 or 20 mmol/L glucose. The data demonstrated that 20 mmol/L glucose stimulated insulin secretion was significantly impaired in KK-Ay mice (3 independent experiments with six to eight mice per genotype). Data are mean±SE. $^*P$ <0.01.

Figure 2. Mitochondrial ultrastructure and number of beta cells. **2A:** Mitochondrial ultrastructure of KK-Ay (right) is severely swollen with disordered cristae, and their number is decreased compared with normal mitochondrial morphology in healthy control (left). Arrows indicate mitochondria. (Original magnification ×30 000. Scale bar equals 500 nm). **2B:** Quantification of total number of mitochondria and average mitochondrial area in healthy and diabetic mice by electron microscopic sections. A total of 50–100 images magnified 10 000× were analyzed. Islets were obtained from six to eight age-matched mice per genotype. Data are mean ± SE. $^*P$ <0.01.

Figure 3. Representative decreased membrane potential (ΔΨm) response to glucose (GS) stimulation in C57BL/6J and KK-Ay beta cells. Cells were dying by Rhodamine 123 (Rh123). **3A:** i means fluorescent intensity (MFI) of beta cells in Krebs-Ringer buffer containing 3 mmol/L glucose; ii MFI responses after 15 minutes of the 20 mmol/L glucose addition, and iii MFI after 10 minutes of 10 mmol/L sodium azide (NaN_3) addition. **3B:** Bar graph illustrates the ΔΨm changes compared with basal levels in KK-Ay and C57BL/6J. Results are the percent change from basal fluorescence (3 mmol/L glucose before additions). Islets were obtained from six to eight age-matched mice per genotype. Data are mean±SE. $^*P$ <0.01.

difference in glucose-induced hyperpolarization of ΔΨm in beta cells from diabetic and control mice which showed a (4.36±1.53)% and (10.90±1.80)% (P <0.01) decrease in hyperpolarization of ΔΨm, respectively, suggesting defective glucose metabolism and mitochondrial function.

Activity of L-type and store-operated Ca^{2+} channels

Beta cells in KK-Ay islets were significantly hypertrophic as determined by resting membrane capacitance (Cm), which serves as a measure of cell size (KK-Ay Cm=(8.93±1.38) pF, n=51, vs. C57BL/6J (7.01±0.67) pF, n=62; P <0.01). Considering the increased size of KK-Ay mouse beta cells, we normalized the peak L-type and SOC amplitudes to the resting Cm. KK-Ay mouse beta cells display increased activity in L-type Ca^{2+} channels and SOC. We used step depolarization (–50 to 60 mV with 10 mV increments) to assess the amplitude and VDCC. This protocol resulted in one inward current component, showing peaks around 0 mV that could be blocked by 10 μmol/L nifedipine (data not shown). These peaks correspond to L-type VDCC. We found that beta cells of KK-Ay mice display prominently enhanced L-type VDCC currents (KK-Ay (–11.96±2.20) pA/pF, n=36 vs. C57BL/6J (–8.57±1.93) pA/pF, n=45, P <0.01) (Figure 4). These results are in agreement with previously published data,[36] but also contradict some results.[37] To detect store-operated Ca^{2+} (SOC), we used thapsigargin and ramp depolarizations (–100 to 100 mV). As shown in Figure 5, SOC has a linear current-voltage relationship. The peak current in beta cells of KK-Ay mice was significantly higher than in C57BL/6J mice (KK-Ay (–1.19±0.12) pA/pF, n=15, vs. C57BL/6J (–0.44±0.07) pA/pF; n=17, P <0.01). We verified that the cells tested were beta cells by single cell PCR (Figure 4E).

Ca^{2+} influx of islets

We used NMT to monitor calcium signaling in response to glucose stimulation (Figure 6). When C57BL/6J islets (41 islets from 8 mice) were exposed to 20 mmol/L glucose, we observed a typical action potential pattern associated with electrophysiological signaling (Figure 6B), with basal efflux reverted transiently into influx, followed by recovery of basal efflux. The recovery efflux was typically higher than the basal level in the C57BL/6J islets. The response of the diabetic model (40 islets from

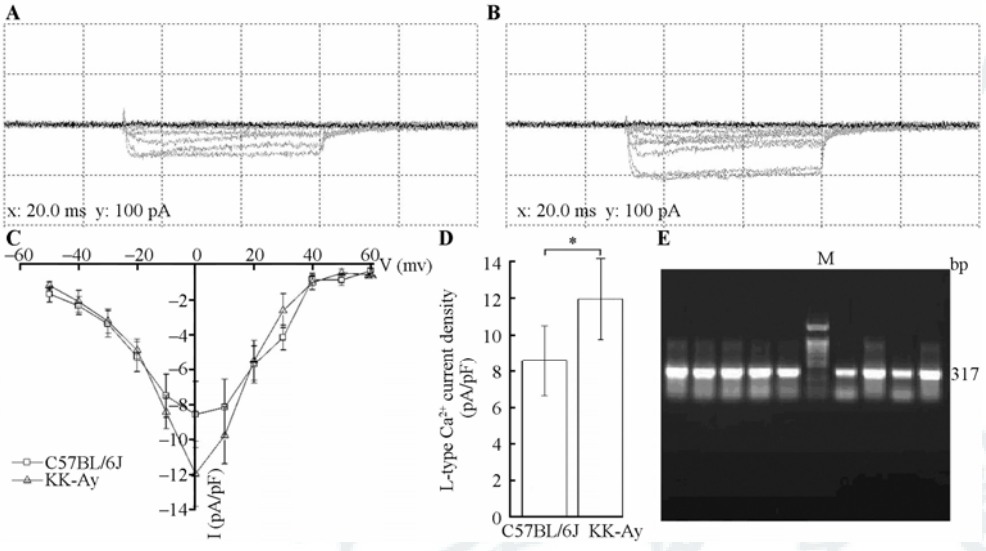

Figure 4. Whole-cell Ca^{2+} currents via L-type Ca^{2+} channels in beta cells. **A** and **B:** Representative sustained inward Ca^{2+} currents were elicited in beta cells of C57BL/6J **(A)** and KK-Ay **(B)**. **C:** I-V curve of beta cells L-type Ca^{2+} currents in C57BL/6J (n=45) and KK-Ay (n=36). Pulses are applied from the holding potential of –70 mV and from –50 to +60 mV with steps of 10 mV. **D:** L-type Ca^{2+} current density of C57BL/6J and KK-Ay mice. **E:** Single cell RT-PCR products from cells with Cm >5 pF. The primer for mouse insulin (317 bp) was used to verify beta cell identity. M represents 100 bp DNA ladder (bottom band=100 bp). Islets were obtained from six to eight age-matched mice per genotype. Data are mean ± SE. $^*P$ <0.01.

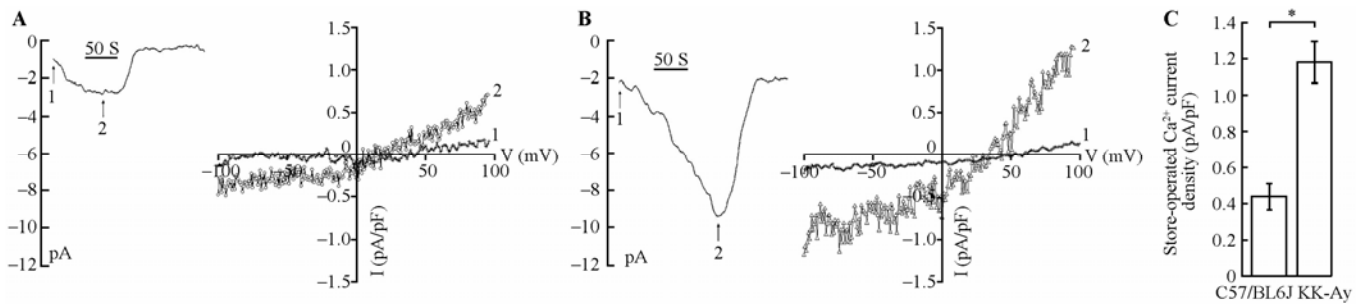

Figure 5. Store operated Ca^{2+} currents of beta cells. **A** and **B:** Whole cell currents elicited by 2 μmol/L Tg in C57BL/6J (**A**) and KK-Ay (**B**). Panels on the left show the I-V curves at two time points. Panels on the right show whole cell currents elicited by Tg at –100 mV. Lines numbered 1 denote the beginning of the experiment. The peak of current induced by Tg is the line numbered 2. **C:** The maximal store operated Ca^{2+} current density of C57BL/6J (n=17) and KK-Ay (n=15) at 100 mV. Islets were obtained from six to eight age-matched mice per genotype. Data are mean±SE. $^*P$ <0.01.

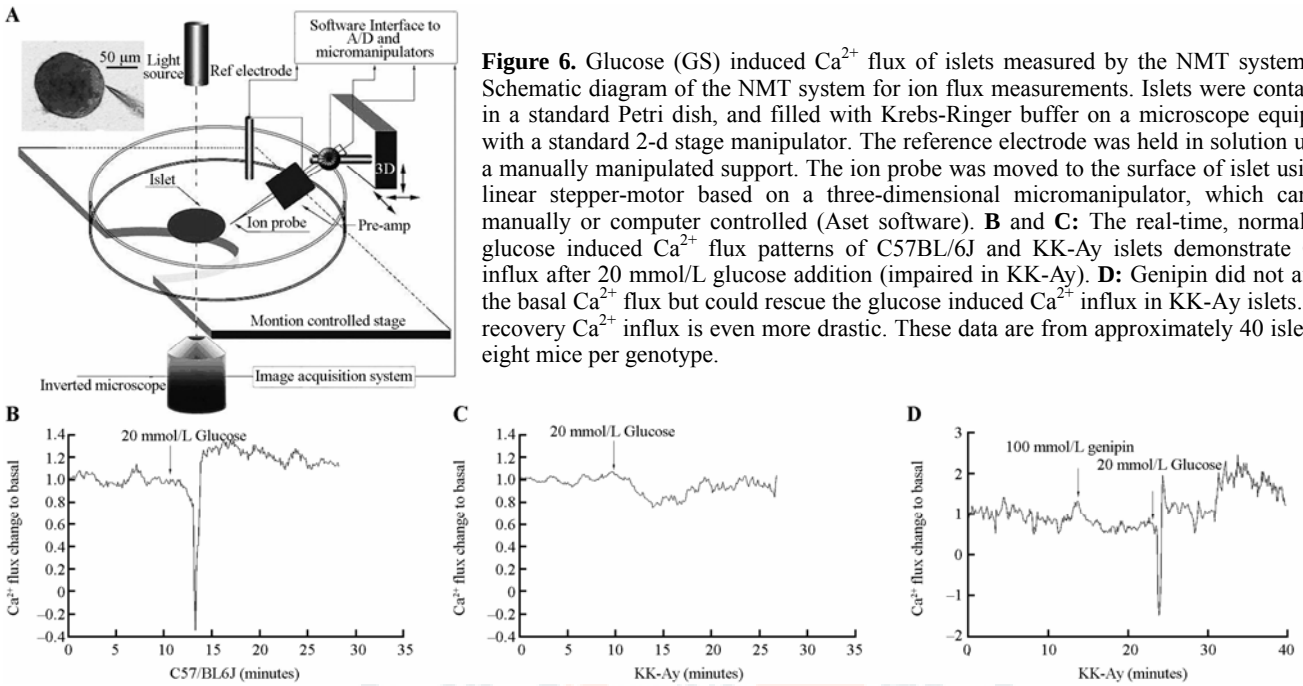

Figure 6. Glucose (GS) induced Ca^{2+} flux of islets measured by the NMT system. **A:** Schematic diagram of the NMT system for ion flux measurements. Islets were contained in a standard Petri dish, and filled with Krebs-Ringer buffer on a microscope equipped with a standard 2-d stage manipulator. The reference electrode was held in solution using a manually manipulated support. The ion probe was moved to the surface of islet using a linear stepper-motor based on a three-dimensional micromanipulator, which can be manually or computer controlled (Aset software). **B** and **C:** The real-time, normalized glucose induced Ca^{2+} flux patterns of C57BL/6J and KK-Ay islets demonstrate Ca^{2+} influx after 20 mmol/L glucose addition (impaired in KK-Ay). **D:** Genipin did not affect the basal Ca^{2+} flux but could rescue the glucose induced Ca^{2+} influx in KK-Ay islets. The recovery Ca^{2+} influx is even more drastic. These data are from approximately 40 islets of eight mice per genotype.

8 mice) deviated from the normal islets in that the response was completely lacking (Figure 6C). To verify the relationship between impaired Ca^{2+} influx and mitochondrial metabolism dysfunction, we rescued the abnormal mitochondrial function in diabetic mice using genipin, which increases mitochondrial membrane potential and increases ATP levels by inhibiting uncoupling protein 2 mediated proton leaks.[38] After addition of 100 μmol/L genipin, the Ca^{2+} flux decreased, but not been significantly compared with the basal flux. We observed a Ca^{2+} influx response pattern similar to the healthy islets following addition of genipin and 20 mmol/L glucose, and the influx and recover flux were more drastic (Figure 6D). This result suggests that Ca^{2+} oscillations in response to glucose in diabetic islets were secondary to abnormal mitochondria metabolism.

DISCUSSION

We characterized mitochondrial morphology, mitochondrial function, Ca^{2+} channel activity, and glucose induced Ca^{2+} influx of islets beta cells in diabetic and healthy mice. The results revealed the following: (1) decreased mitochondrial function and morphology occurs in the beta cells of diabetic mice; (2) increased activities of L-type voltage operated Ca^{2+} channels and store operated Ca^{2+} influx, but impaired glucose induced Ca^{2+} influx in diabetic islets; and (3) glucose induced Ca^{2+} influx in diabetic islets can be rescued after acutely reversing mitochondrial function; even if this influx is more drastic than in the healthy islets.

It has been suggested that defective glucose metabolism may be an upstream contributory element leading to impaired insulin secretion, whereas the secretory machinery itself may not be directly affected.[39] In this study, we used diabetic KK-Ay mice, which have been frequently used as an animal model for noninsulin-dependent diabetes.[40,41] The symptoms in these mice are similar to diabetic patients, in that they exhibit metabolic abnormalities, such as an absolute or relative lack of insulin, hyperglycemia and glucose intolerance, and elevated lipids. Our results suggest that the altered Ca^{2+} oscillation in type 2 diabetic mice is caused by abnormal mitochondrial activation and directly verified the Ca^{2+} influx change of diabetic and healthy islets under glucose stimulation, but not the Ca^{2+} channels activity.

Abnormal mitochondrial function has been associated with beta cell dysfunction in type 2 diabetes in previous studies. Mitochondria structural changes typically parallel their functional state in both physiological as well as pathological conditions.[42] Using electron microscopy examination, our study reveals clear morphological defects in beta cell mitochondria. Consistent with abnormalities in mitochondrial morphology, we found that glucose-induced hyperpolarization of mitochondrial membranes was reduced in islets from diabetic subjects compared with controls. Our finding is in agreement with previous studies that showed lower glucose-induced $\Delta\Psi m$ in islets from human type 2 diabetic patients and diabetic animal model.

Ca^{2+} channel activity should first be considered when Ca^{2+} oscillation is abnormal in diabetic beta cells. In a previous GSIS model, it was simply corresponded that the closure of K_{ATP} channels caused the membrane depolarization. However, the mechanism by which membrane depolarization activates L-type Ca^{2+} channels is very complex, and somewhat misunderstood because of the tendency to oversimplify. And K_{ATP} channels can not

support such a strong membrane depolarization solely because a background K^+ current are need to maintain the membrane potential. Hence, at least one additional depolarizing component exists in beta cells.[43] Further research suggested that the SOC contribute to membrane potential and provides the basis for Ca^{2+} entry and has a critical relationship with GSIS in primary mouse beta cells.[44] Thus, we performed whole-cell patch-clamp recording to investigate both L-type and SOC Ca^{2+} current. Our results indicate that both L-type and SOC Ca^{2+} channel activities are increased in beta cells of KK-Ay mice. This finding is compatible with observations that L-type Ca^{2+} channel activities are enhanced in beta cells of GK and NSZ rats. We additionally found that diabetic cells are significantly hypertrophic. As secretary capacity of single beta cells is positively correlated to cell size, beta cell hypertrophy is generally believed to enhance secretion to cope with the increased secretory demand during hyperglycemia.

Except for the effect of Ca^{2+} channels, we investigated the glucose induced Ca^{2+} influx of beta cells in islets. Islets are heterogeneous cell aggregates containing beta cells (70%–80%), alpha cells (10%–15%), and delta cells (5%–10%). No metabolic responses are evident when alpha cells are challenged with glucose,[45] such that signals of ionic changes are beta cell dominated. Previous studies suggest that the secretary capacity of beta cells are particularly dependent on functional interaction between cells within islets [46] and is negatively affected by cell culture and isolation. Other studies have demonstrated differences in the physiological behavior when data from dispersed cultured islet cells and fresh intact islets are compared. The latter model is likely closer to the physiological scenario.[47] Ca^{2+} fluorescent dye is a commonly used to investigate Ca^{2+} oscillation. The NMT method is also an ideal technique that can directly measure the magnitude and direction of Ca^{2+} flux across membranes in situ, with a high level of temporal and spatial resolution. Our data demonstrated a three-step electrophysiological Ca^{2+} signaling event associated with glucose stimulation in healthy islets: basal efflux, transient influx, and recovery of basal efflux. The basal efflux presents the general Ca^{2+} efflux by Na^+/Ca^{2+} exchange in the membrane. The transient influx accounts for the majority of L-type Ca^{2+} channel activation by glucose stimulation. The recovery efflux response is to recover the normal concentration of intracellular calcium by the secretory granules exocytosed. Compared with healthy islets, we found the glucose induced Ca^{2+} influx and the glucose induced Ca^{2+} efflux were decreased significantly in diabetic islets. The whole-cell patch-clamp results, combined with increased Ca^{2+} channel activity, but decreased glucose induced Ca^{2+} influx, suggests a new putative mechanism. Mitochondrial function was impaired with age and/or nutrient overloading, which decreased signals to drive membrane depolarization. In contrast, mitochondrial dysfunction in peripheral tissues, such as skeleton muscle and liver, will cause hyperglycemia and insulin resistance. Thus, the relative demand for insulin increased, which induced beta cells to enlarge. The increased activity of L-type and store-operated Ca^{2+} channel activities should correspond to increased expression levels. The upregulated activity and expression level of L-type and store-operated Ca^{2+} channels activities should correspond to this. So after genipin rescued the mitochondrial function accurately, we found glucose induced Ca^{2+} influx and the following Ca^{2+} efflux were recovered and the change was more drastic.

In conclusion, the present data indicate that in pancreatic beta cells from KK-Ay mice, the impaired insulin secretory response to glucose is associated with a marked abnormal Ca^{2+} influx caused by impaired mitochondrial function, but not the Ca^{2+} channels activity. The data regarding a role for mitochondria affecting calcium in insulin secretion is both predictable, and yet compelling, in terms of the physiological and pathological mechanisms of diabetes.

REFERENCES

1. Bell GI, Polonsky KS. Diabetes mellitus and genetically programmed defects in beta-cell function. Nature 2001; 414: 788-791.
2. Kahn SE. The relative contributions of insulin resistance and beta-cell dysfunction to the pathophysiology of type 2 diabetes. Diabetologia 2003; 46: 3-19.
3. Jensen CC, Cnop M, Hull RL, Fujimoto WY, Kahn SE. Beta-cell function is a major contributor to oral glucose tolerance in high-risk relatives of four ethnic groups in the U.S. Diabetes 2002; 51: 2170-2178.
4. Maechler P, Wollheim CB. Mitochondrial function in normal and diabetic beta-cells. Nature 2001; 414: 807-812.
5. Pertusa JA, Nesher R, Kaiser N, Cerasi E, Henquin JC, Jonas JC. Increased glucose sensitivity of stimulus-secretion coupling in islets from Psammomys obesus after diet induction of diabetes. Diabetes 2002; 51: 2552-2560.
6. Liu YJ, Grapengiesser E, Gylfe E, Hellman B. Crosstalk between the cAMP and inositol trisphosphate-signalling pathways in pancreatic beta-cells. Arch Biochem Biophys 1996; 334: 295-302.
7. Dyachok O, Gylfe E. Ca^{2+}-induced Ca^{2+} release via inositol 1,4,5-trisphosphate receptors is amplified by protein kinase A and triggers exocytosis in pancreatic beta-cells. J Biol Chem 2004; 279: 45455-45461.
8. Dyachok O, Tufveson G, Gylfe E. Ca^{2+}-induced Ca^{2+} release by activation of inositol 1,4,5-trisphosphate receptors in primary pancreatic beta-cells. Cell Calcium 2004; 36: 1-9.
9. Liu YJ, Gylfe E. Store-operated Ca^{2+} entry in insulin-releasing pancreatic beta-cells. Cell Calcium 1997; 22: 277-286.
10. Valdeolmillos M, Nadal A, Contreras D, Soria B. The relationship between glucose-induced K^+_{ATP} channel closure and the rise in $[Ca^{2+}]i$ in single mouse pancreatic beta-cells. J Physiol 1992; 455: 173-186.
11. Silva JP, Kohler M, Graff C, Oldfors A, Magnuson MA,

Berggren PO, et al. Impaired insulin secretion and beta-cell loss in tissue-specific knockout mice with mitochondrial diabetes. Nat Genet 2000; 26: 336-340.
12. Maassen JA, LM TH, Van Essen E, Heine RJ, Nijpels G, Jahangir Tafrechi RS, et al. Mitochondrial diabetes: molecular mechanisms and clinical presentation. Diabetes 2004; 53 Suppl 1: s103-s109.
13. Benninger RK, Remedi MS, Head WS, Ustione A, Piston DW, Nichols CG. Defects in beta cell Ca^{2+} signalling, glucose metabolism and insulin secretion in a murine model of K(ATP) channel-induced neonatal diabetes mellitus. Diabetologia 2011; 54: 1087-1097.
14. Benninger RK, Remedi MS, Head WS, Ustione A, Piston DW, Nichols CG. Defects in beta cell Ca^{2+} signalling, glucose metabolism and insulin secretion in a murine model of K_{ATP} channel-induced neonatal diabetes mellitus. Diabetologia 2011; 54: 1087-1097.
15. Anello M, Lupi R, Spampinato D, Piro S, Masini M, Boggi U, et al. Functional and morphological alterations of mitochondria in pancreatic beta cells from type 2 diabetic patients. Diabetologia 2005; 48: 282-289.
16. Del Guerra S, Lupi R, Marselli L, Masini M, Bugliani M, Sbrana S, et al. Functional and molecular defects of pancreatic islets in human type 2 diabetes. Diabetes 2005; 54: 727-735.
17. Lu H, Koshkin V, Allister EM, Gyulkhandanyan AV, Wheeler MB. Molecular and metabolic evidence for mitochondrial defects associated with beta-cell dysfunction in a mouse model of type 2 diabetes. Diabetes 2010; 59: 448-459.
18. Luciani DS, Ao P, Hu X, Warnock GL, Johnson JD. Voltage-gated Ca^{2+} influx and insulin secretion in human and mouse beta-cells are impaired by the mitochondrial Na^{+}/Ca^{2+} exchange inhibitor CGP-37157. Eur J Pharmacol 2007; 576: 18-25.
19. Li F, Zhang ZM. Comparative identification of Ca^{2+} channel expression in INS-1 and rat pancreatic beta cells. World J Gastroenterol 2009; 15: 3046-3050.
20. Schulla V, Renstrom E, Feil R, Feil S, Franklin I, Gjinovci A, et al. Impaired insulin secretion and glucose tolerance in beta cell-selective Ca(v)1.2 Ca^{2+} channel null mice. Embo J 2003; 22: 3844-3854.
21. Tamarina NA, Kuznetsov A, Philipson LH. Reversible translocation of EYFP-tagged STIM1 is coupled to calcium influx in insulin secreting beta-cells. Cell Calcium 2008; 44: 533-544.
22. Lin JM, Fabregat ME, Gomis R, Bergsten P. Pulsatile insulin release from islets isolated from three subjects with type 2 diabetes. Diabetes 2002; 51: 988-993.
23. Rose T, Efendic S, Rupnik M. Ca^{2+}-secretion coupling is impaired in diabetic Goto Kakizaki rats. J Gen Physiol 2007; 129: 493-508.
24. Quesada I, Nadal A, Soria B. Different effects of tolbutamide and diazoxide in alpha-, beta-, and delta-cells within intact islets of Langerhans. Diabetes 1999; 48: 2390-2397.
25. Quesada I, Rovira JM, Martin F, Roche E, Nadal A, Soria B. Nuclear KATP channels trigger nuclear Ca^{2+} transients that modulate nuclear function. Proc Natl Acad Sci U S A 2002; 99: 9544-9549.
26. Takahashi A, Motomura K, Kato T, Yoshikawa T, Nakagawa Y, Yahagi N, et al. Transgenic mice overexpressing nuclear SREBP-1c in pancreatic beta-cells. Diabetes 2005; 54: 492-499.
27. da Silva Xavier G, Loder MK, McDonald A, Tarasov AI, Carzaniga R, Kronenberger K, et al. TCF7L2 regulates late events in insulin secretion from pancreatic islet beta-cells. Diabetes 2009; 58: 894-905.
28. Barg S, Galvanovskis J, Gopel SO, Rorsman P, Eliasson L. Tight coupling between electrical activity and exocytosis in mouse glucagon-secreting alpha-cells. Diabetes 2000; 49: 1500-1510.
29. Rabe H, Ritz HJ, Jeserich G. Voltage-gated potassium channels of Schwann cells from trout lateral line nerve: a combined electrophysiological and molecular characterization. Glia 1998; 23: 329-338.
30. Kuhtreiber WM, Jaffe LF. Detection of extracellular calcium gradients with a calcium-specific vibrating electrode. J Cell Biol 1990; 110: 1565-1573.
31. Xu Y, Sun T, Yin LP. Application of non-invasive microsensing system to simultaneously measure both H^{+} and O_2 fluxes around the pollen tube. J Integr Plant Biol 2006; 48: 823-831.
32. Porterfield DM, Corkey RF, Sanger RH, Tornheim K, Smith PJ, Corkey BE. Oxygen consumption oscillates in single clonal pancreatic beta-cells (HIT). Diabetes 2000; 49: 1511-1516.
33. Gleichmann M, Collis LP, Smith PJ, Mattson MP. Simultaneous single neuron recording of O_2 consumption, $[Ca^{2+}]i$ and mitochondrial membrane potential in glutamate toxicity. J Neurochem 2009; 109: 644-655.
34. Zhao M, Song B, Pu J, Wada T, Reid B, Tai G, et al. Electrical signals control wound healing through phosphatidylinositol-3-OH kinase-gamma and PTEN. Nature 2006; 442: 457-460.
35. McLamore ES, Porterfield DM, Banks MK. Non-invasive self-referencing electrochemical sensors for quantifying real-time biofilm analyte flux. Biotechnol Bioeng 2009; 102: 791-799.
36. Kato S, Ishida H, Tsuura Y, Tsuji K, Nishimura M, Horie M, et al. Alterations in basal and glucose-stimulated voltage-dependent Ca^{2+} channel activities in pancreatic beta cells of non-insulin-dependent diabetes mellitus GK rats. J Clin Invest 1996; 97: 2417-2425.
37. Hughes SJ, Faehling M, Thorneley CW, Proks P, Ashcroft FM, Smith PA. Electrophysiological and metabolic characterization of single beta-cells and islets from diabetic GK rats. Diabetes 1998; 47: 73-81.
38. Zhang CY, Parton LE, Ye CP, Krauss S, Shen R, Lin CT, et al. Genipin inhibits UCP2-mediated proton leak and acutely reverses obesity- and high glucose-induced beta cell dysfunction in isolated pancreatic islets. Cell Metab 2006; 3: 417-427.
39. Abdel-Halim SM, Guenifi A, Khan A, Larsson O, Berggren PO, Ostenson CG, et al. Impaired coupling of glucose signal to the exocytotic machinery in diabetic GK rats: a defect ameliorated by cAMP. Diabetes 1996; 45: 934-940.
40. Liu J, Sun H, Duan W, Mu D, Zhang L. Maslinic acid reduces blood glucose in KK-Ay mice. Biol Pharm Bull 2007; 30: 2075-2078.
41. Ribnicky DM, Poulev A, Watford M, Cefalu WT, Raskin I.

Antihyperglycemic activity of Tarralin, an ethanolic extract of Artemisia dracunculus L. Phytomedicine 2006; 13: 550-557.
42. Wakabayashi T. Megamitochondria formation—physiology and pathology. J Cell Mol Med 2002; 6: 497-538.
43. Rorsman P, Eliasson L, Renstrom E, Gromada J, Barg S, Gopel S. The cell physiology of biphasic insulin secretion. News Physiol Sci 2000; 15: 72-77.
44. Miura Y, Henquin JC, Gilon P. Emptying of intracellular Ca^{2+} stores stimulates Ca^{2+} entry in mouse pancreatic beta-cells by both direct and indirect mechanisms. J Physiol 1997; 503(Pt 2): 387-398.
45. Quesada I, Todorova MG, Soria B. Different metabolic responses in alpha-, beta-, and delta-cells of the islet of Langerhans monitored by redox confocal microscopy. Biophys J 2006; 90: 2641-2650.
46. Speier S, Gjinovci A, Charollais A, Meda P, Rupnik M. Cx36-mediated coupling reduces beta-cell heterogeneity, confines the stimulating glucose concentration range, and affects insulin release kinetics. Diabetes 2007; 56: 1078-1086.
47. Fernandez J, Valdeolmillos M. Synchronous glucose-dependent $[Ca^{2+}]$i oscillations in mouse pancreatic islets of Langerhans recorded *in vivo*. FEBS Lett 2000; 477: 33-36.

(Received August 11, 2011)
Edited by GUO Li-shao